Journal of Alloys and Compounds 504S (2010) S389–S394

Contents lists available at ScienceDirect

Journal of Alloys and Compounds

journal homepage: www.elsevier.com/locate/jallcom

Production and dispersion stability of ultrafine Al–Cu alloy powder in base fluid

S. Samal, B. Satpati [1], D. Chaira *

National Institute of Technology, Rourkela, India

ARTICLE INFO

Article history:
Received 2 July 2009
Received in revised form 23 March 2010
Accepted 31 March 2010
Available online 7 April 2010

Keywords:
Nanostructured materials
Mechanical alloying
Powder metallurgy
X-ray diffraction
Scanning electron microscope
Transmission electron microscope

ABSTRACT

In the present investigation, high-energy milling was carried out to synthesize ultrafine Al–Cu alloy powder from elemental Al and Cu powder. Elemental Al and Cu powders were milled in a high-energy planetary mill at a speed of 300 rpm and at 10:1 ball to powder weight ratio. Milling was carried out for 50 h in wet condition to prevent undue oxidation and agglomeration. Powder particles were characterized by X-ray diffraction (XRD), particle size analyzer, scanning electron microscope (SEM), and transmission electron microscope (TEM). It is found from XRD that nanostructured Al–Cu alloy prepared by high-energy milling resulted in a grain size of around 6.0 nm and lattice strain of about 1.43%. It is also found that the average particle size is around 4.0 μm after 50 h of milling. TEM shows that particles are irregular in shape and their size is around 200–300 nm. To study the dispersion stability, alloy powders were dispersed in de-ionized water and then zeta potential were measured at different pHs. The zeta potential value of the Al–Cu dispersion increases numerically from 49.00 (pH 4.96) to −90.60 (pH 9.50) when oleic acid is added. It is evident from different zeta potential values that stability is improved by the addition of oleic acid into the dispersion.

1. Introduction

Nanofluids have attracted attention as a new generation of heat transfer fluids with superior potential for enhancing the heat transfer performance of conventional fluids. These fluids are obtained by a stable colloidal suspension of low volume fraction of ultrafine solid particles in nanometric dimension dispersed in conventional heat transfer fluid such as water, ethylene glycol or propylene glycol in order to enhance or improve its rheological, optical, and thermal properties. The concept of nanofluid was first coined by Choi [1] at Argonne National Laboratory for heat transfer applications [2]. It was found by several researchers that the thermal conductivity of these fluids can be significantly increased when compared to the same fluids without nanoparticles. Since thermal conductivity of solids is orders of magnitude greater than that of liquids, dispersion of solid particles in a given fluid is bound to increase its thermal conductivity. The dispersion of a low volume (<1%) fraction of solid nanoparticles in traditional base fluid drastically increases the thermal conductivity than that of base fluid [3,4]. The much larger surface areas of nanoparticles relative to those of micro/macro-sized particles should not only improve heat transfer capabilities, but also increase the stability of the suspensions. Lee et al. [5] demonstrated a maximum increase in the thermal conductivity of approximately 20% when CuO nanoparticles were suspended in ethylene glycol. Eastman et al. [6] were able to increase the thermal conductivity of ethylene glycol up to 40% by suspending copper nanoparticles (average diameter less than 10 nm). In the same year, Choi et al. [7] reported 160% increase of a synthetic poly oil thermal conductivity when metallic multi-wall nanotubes were suspended. Das et al. [8] observed that the thermal conductivity for nanofluid increases with increasing temperature.

The enhancement of thermal conductivity of nanofluid over conventional base fluid like de-ionized water, ethylene glycol, etc. has several applications starting from closely packed integrated circuits at small scale industry to nuclear reactor at large scale. However, dispersion of milli- and micrometer-sized particles is prone to sedimentation, clogging and erosion of pipes and channels. The nanofluid is stable, introduce very little pressure drop and it can pass through nanochannels [9]. The stability of suspension is one of the crucial factors required for improving the thermal conductivity of the fluid and its applications as an efficient coolant [10].

There are two techniques for production of nanofluids: (i) the one-step direct evaporation method [11–14] represents the direct formation of the nanoparticles in the base fluid and (ii) the two-step method [3,4] represents the formation of nanoparticles and subsequent dispersion of the nanoparticles in the base fluid. In either of the case, the production of a uniformly dispersed nanofluid is essential for obtaining stable and superior properties of nanofluids [15,7]. Several techniques have been developed to synthesize nanoparticles such as co-precipitation [16–18], sonochemical technique [19],

* Corresponding author at: National Institute of Technology Rourkela, Bhubaneswar, Orissa, India. Tel.: +91 9438370956.
E-mail address: chaira.debasis@gmail.com (D. Chaira).
[1] Institute of Minerals and Materials Technology, Bhubaneswar, Orissa, India.

0925-8388/$ – see front matter © 2010 Elsevier B.V. All rights reserved.
doi:10.1016/j.jallcom.2010.03.223

Table 1
The specifications for the milling systems.

Mill type	Fritsch planetary mill
Milling time	50 h
Wet milling	Media toluene
Milling speed	300 rpm
Grinding media	
Type	Steel
Ball size	9.30 mm (dia.)
Ball weight/jar	350 g
Ball to powder ratio by weight	10
Jar dimensions	
Length	95 mm
Diameter	75 mm
Jar speed	300 rpm

sol–gel [20] and hydrothermal [21], etc. A two-step approach has been adopted here to prepare ultrafine dispersion of Al–Cu powder particles. Al–Cu system is chosen in order to take the advantages of both thermal conductivity and dispersion stability. Al has lower density than Cu, i.e. Al ultrafine particles will suspend at higher altitude in base fluid than Cu. So dispersion stability will be good in case of Al but Cu has higher thermal conductivity than Al. Here, the ultrafine particles were prepared by high-energy milling (HEM) [22,23] with the help of a Fritsch pulverisette-5 planetary ball mill. High-energy ball induces high-energy impact on the charged powder by collision between balls and powder causing severe plastic deformation, repeated fracturing and cold welding of charged powder leading to the formation of nanoparticles [24–26]. The prepared ultrafine particles were then dispersed into de-ionized water using ultrasonic probe and magnetic stirrer to prepare desired suspension.

Although many experimental studies on nanofluid systems have been performed, the preparation methods for stable nanofluid were not systematically studied yet. In earlier study, stability of carbon black- and silver-based nanofluid was studied by Kim and colleagues [27]. Chang and Chang [28] studied the suspension stability of Al_2O_3 nanofluid with different pHs. Kim et al. [29] studied the effect of sonication on zeta potential value of CuO particles. In the present study, the primary objectives are to synthesize ultrafine Al–Cu alloy powder particles and preparation of stable dispersion of ultrafine particles in base fluid to develop heat transfer fluids.

2. Experimental

Milling was carried out in Pulverisette-5 planetary ball mill with steel vials and steel balls. Starting materials used for milling were elemental Al and Cu powder with 99% purity. The ball to powder weight ratio (BPR) was 10:1. Milling was conducted at 300 rpm in wet medium (about 50 ml of toluene) to prevent undue oxidation and agglomeration of powder. Powder particles were milled for 50 h in two vials—each containing 35 g powder and 350 g steel balls. Steel balls of diameter 10 mm were used for milling. Powder samples were picked up from the vials after selected interval of milling time to see the change in shape and size reduction of powder samples. Powders were characterized by X-ray diffraction (XRD), particle size analyzer, scanning electron microscopy (SEM) and transmission electron microscopy (TEM). The specifications of milling system are provided in Table 1.

A very small amount of milled powders (approximately 0.04 g) were dispersed in de-ionized water (150 ml) by ultrasonication and subsequently magnetic stirring for about 30 min each to prepare the desired suspension. The pH was controlled using acetic acid and ammonium hydroxide. The prepared dispersions were analyzed by nano-zeta meter to determine the particle size and to study the stability of suspensions at a particular pH value with and without surfactant by measuring zeta potential. The sequence of steps for preparation of dispersion is given in Table 2.

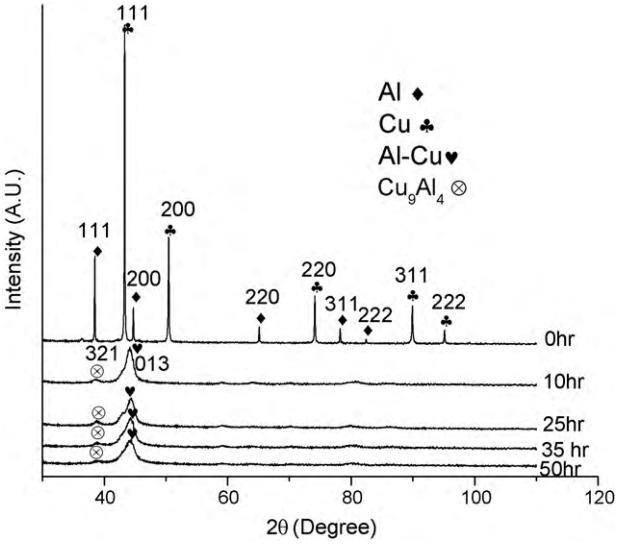

Fig. 1. The XRD patterns of Al–Cu powder particles at different intervals of milling time.

3. Results and discussion

3.1. Characterization of Al–Cu ultrafine particles

3.1.1. X-ray diffraction (XRD) analysis

To study the different phase evolutions during milling, XRD of powder milled for different time period was conducted. The XRD pattern of mixture of Al and Cu powder particles at different intervals of milling time is shown in Fig. 1. The XRD pattern of as received powder shows the individual peak of Cu and Al. The final milling product is a single-phase nanocrystalline material which is clear from the graph. It is evident from the figure that after 10 h of milling, Al–Cu alloy has started to form. The figure shows that the Bragg peaks for milled product (after 50 h of milling) are broad, suggesting accumulation of lattice strain and reduction in crystallite size. It is also observed that intensity of the individual peaks decreases due to the decrease of crystallinity of powder during milling.

3.1.2. Crystallite size and lattice strain measurement

The crystallite size can be investigated by analyzing the X-ray diffraction patterns. For this purpose, as received and milled powders were analyzed using X-ray diffraction (XRD) methods with CuKα radiation. The XRD peak broadening was used to measure the crystallite size and lattice strain. The Philips X'pert High Score software has been used here to calculate the crystallite size and lattice strain.

The decrease of the grain size and lattice strain to characterize the activation process has been determined from the X-ray

Table 2
The methods of producing suspensions.

Two-step method of producing	Test conditions	Al–Cu–water
Al–Cu suspensions		
Magnetic stirrer	Revolution speed: 1500 rpm Revolution time: 30 min	Weight of powder: 0.04 g Base fluid: DI-water
Ultrasonic disruptor	Sonication time: 30 min Frequency: 20 kHz Maximum sonicating power: 350 W	Viscosity of DI-water: 0.87 mm^2/s Surfactant: oleic acid

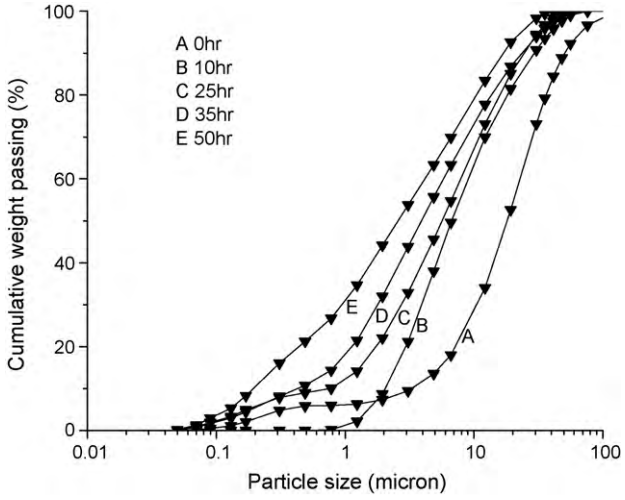

Fig. 2. Particle size distribution of Al–Cu powder at different intervals of milling time.

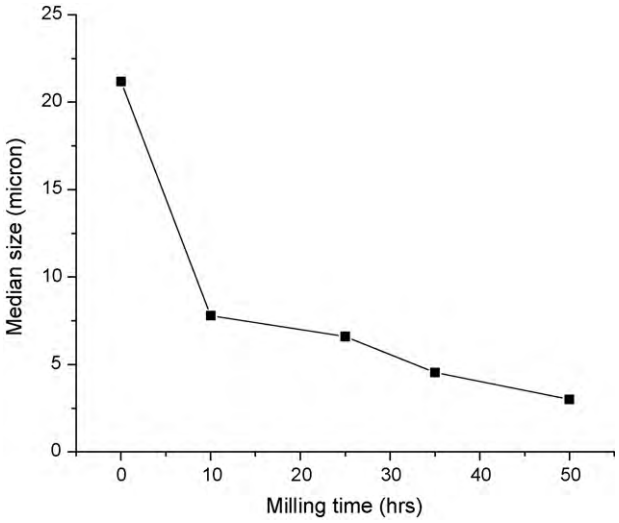

Fig. 3. Variation of average Al–Cu particle size with milling time.

diffraction patterns. Although the accumulation of lattice strain is a measure of defect formation, determining the defect structure was found to be more difficult. The crystallite size and the lattice strain of the mixture of Al and Cu powder measured from the XRD peak broadening is shown as a function of milling time in Table 3. It can be seen that the crystallite size decreases and internal strain increases with milling time. After 10 h of milling, crystal size is around 21 nm which reduces to 6 nm after 50 h of milling, whereas lattice strain is increased from 0.435 to 1.434%.

3.1.3. Particle size analysis

During mechanical alloying process, powder morphology and size change continuously. The particle size of mixture of Al and Cu powder was measured by Malvern particle size analyzer. During the early stage of milling, the powder particles of Al and Cu (50 at.%) were mixed together and then mechanically alloyed such that individual particles of Al and Cu could form nanocrystalline material. At a later stage, after about 10 h of milling, the solid state reaction starts and considerable amounts of the product (Al–Cu) are formed. Fig. 2 shows the particle size distribution of powder at different intervals of milling time. The average particle size of powder particles is shown in Fig. 3. It is evident from the figure that average particle size has been reduced from initial size 21–3 μm after 50 h of milling. There was no evidence of welding, as particle size did not increase during the initial stages of milling. It should be mentioned that the size spectra corresponding to individually milled product of Al and Cu did not show any evidence of growth in particle size.

Particle size of the final milled powder (50 h) has also been measured by nanoparticle size analyzer. Particle size of the final milled powder (50 h) measured by nanoparticle size analyzer has been shown in Fig. 4. The figure shows that particle size distribution is a bi-modal kind of distribution which indicates that in one mode of size distribution particles are observed up to around 1500 nm and in another mode of distribution size ranges from 3000 to 7000 nm. The particle size distribution shows wide size distribution of particles.

Table 3
Variation of crystallite size and lattice strain with milling time for Al–Cu alloy.

Milling time	Crystallite size (nm)	Lattice strain (%)
10 h	21	0.435
25 h	11	0.815
35 h	9	1.028
50 h	6	1.434

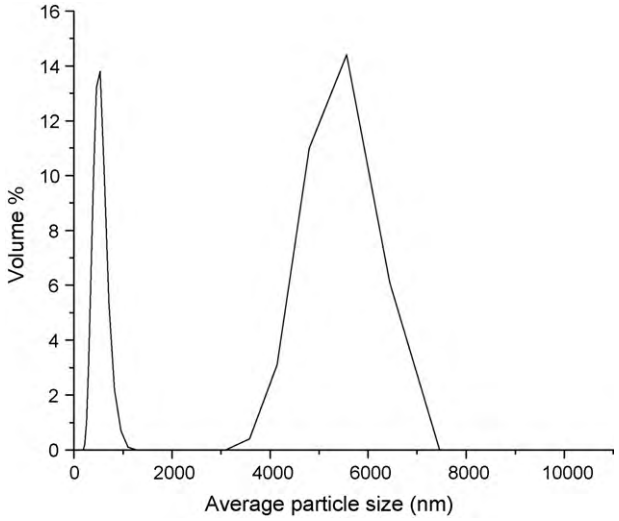

Fig. 4. Particle size distribution of Al–Cu powder–de-ionized water-based suspension.

3.1.4. Scanning electron microscopy (SEM) study

The morphology and size of initial powders and also milled powders after different intervals of milling time were investigated with the help of scanning electron microscopy (SEM). The marker is set at 10 μm. Fig. 5 shows the SEM micrographs of mixture of Al and Cu powder milled for different milling times. The micrographs show that powders of reacting materials are bulky with random shape and size at the initial stage of milling. The size of initial powders is around 28 μm. As the milling progresses the powders become more homogeneous. As regards particle size, it is also evident from the SEM images that it decreases gradually with increasing milling time. However, no evidence of particle coarsening could be obtained through SEM. The qualitative chemical analysis of Al–Cu powder milled for 50 h was carried out using energy dispersive X-ray analysis. The elemental analysis of Al–Cu alloy measured by EDS is shown in Table 4. Milling was carried out in open atmosphere, some oxide has been formed. As steel jars and steel balls were used, some carbon contamination is there. Carbon mainly comes from carbon tape as powder was dispersed into carbon tape. Since stainless steel contains very few percents of carbon. Although EDS shows the presence of C and O_2, but XRD cannot detects the same, as their amount is very low.

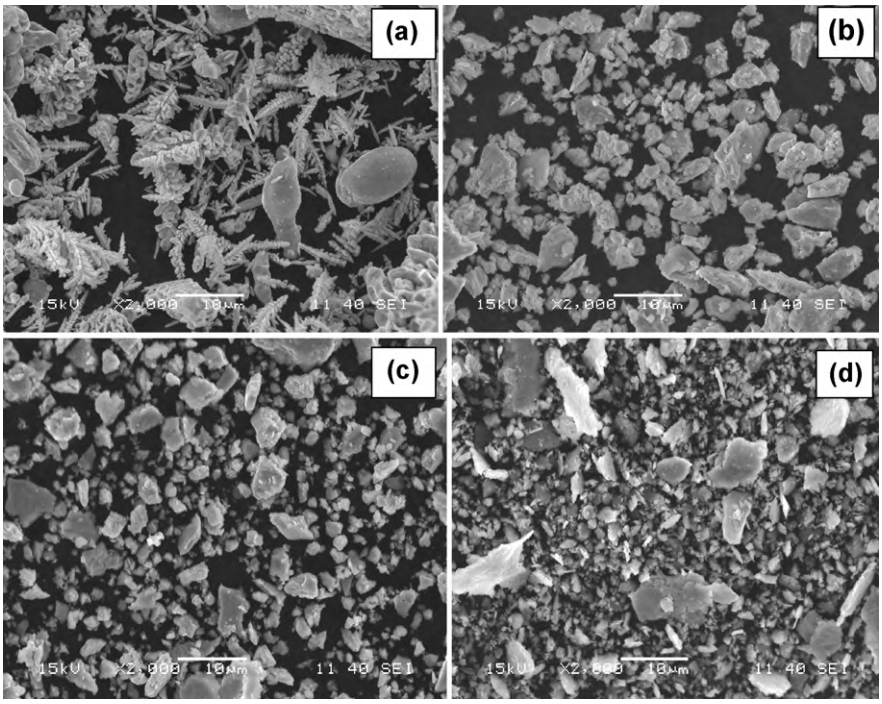

Fig. 5. SEM micrographs of Al–Cu milled powder: (a) 0 h, (b) 10 h, (c) 25 h and (d) 50 h.

Table 4
Elemental analysis of 50 h milled Al–Cu alloy.

Elements	Weight %
C	18.69
O	8.95
Al	17.50
Cu	54.87

3.1.5. Transmission electron microscopy (TEM) study

The internal structure and the true particle size of the mechanically alloyed powders were investigated by TEM. The sample for TEM was prepared by adding a pinch of milled alloy powder particles in the beaker containing acetone and kept in an ultrasonic bath for about 15 min to get uniform dispersion of powder particles in the liquid. After that 2 drops of fluid containing dispersed particles were added in carbon coated Cu-grid and then dried. The desired sample was fixed in the sample holder of TEM for analyzing the internal structure of mechanically alloyed powder. Fig. 6 shows the bright field TEM micrograph and corresponding SAD pattern of 50 h milled powders. It is evident from the figure that the particle size is around 200–400 nm and contains large number of crystallites (size around 15–20 nm) with difference in contrast due to the variation of orientation. The SAD pattern for Al–Cu alloy is slightly diffused hallow which indicates that powder particles are partial amorphous in nature.

3.2. Dispersion stability of Al–Cu ultrafine particles in basefluid

The stability of the dispersion was determined by measuring zeta potential values of alloy powder dispersed in de-ionized water. However, for measurement of zeta potential, dilute fraction of alloy suspension was selected here. The values of zeta potential ζ can be

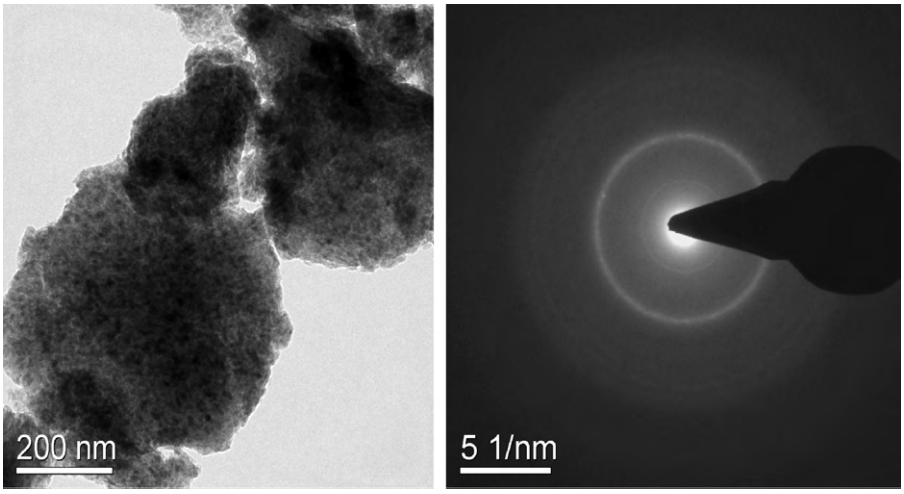

Fig. 6. Bright field TEM micrograph and corresponding SAD pattern: Al–Cu.

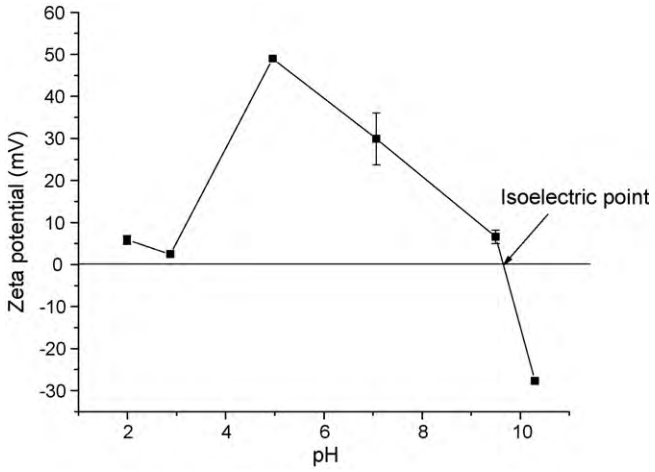

Fig. 7. The evolution of zeta potentials of the de-ionized water-Al–Cu alloy powder suspension as a function of pH without surfactant.

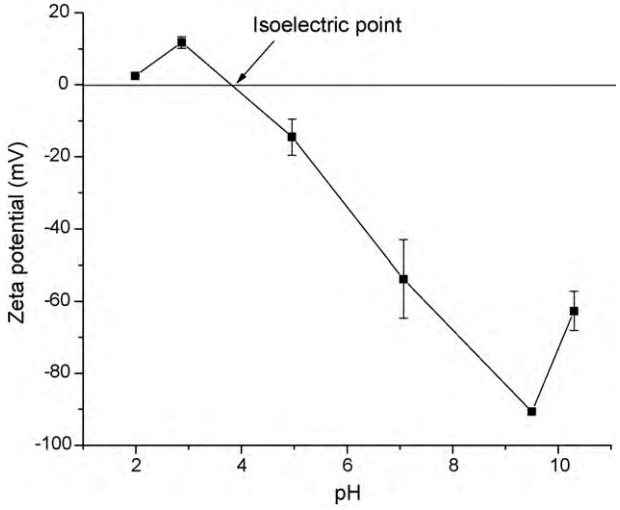

Fig. 8. The evolution of zeta potentials of the de-ionized water-Al–Cu alloy powder suspension as a function of pH with surfactant.

calculated by the Helmholtz–Smoluchowski equation.

$$\zeta = \frac{\mu \cup}{\varepsilon}$$

where $\cup$ is the electrophoretic mobility, and μ, ε are the viscosity and the dielectric constant of the liquid in the boundary respectively.

The zeta potential is zero at pH 9.70, which is isoelectric point as shown in Fig. 7. Therefore the force of electrostatic repulsion between particles is not sufficient to overcome the attraction force between the particles and hence the dispersion is least stable. As pH increases or decreases by adding reacting reagent ammonium hydroxide (NH_4OH) or acetic acid respectively, then the particles tend to acquire more charge, so the electrostatic repulsion force between the particles becomes sufficient to prevent attraction and collision between particles caused by Brownian motion. Greater electrostatic force can also lead to more free particles by increasing particle–particle distance so that the distance exceeds the hydrogen bonding range between particles and further reduces the probability of particle coagulation and settling and hence improving the dispersion stability of Al–Cu alloy.

At pH 10.30 and 4.96, the zeta potential becomes higher; the electrostatic repulsion force between the particles is stronger, and the coagulated particles can redisperse through mechanical force. Therefore the dispersion stability of Al–Cu alloy is best at pH 4.96 and 10.30 corresponding to zeta potential values of 49 and −27.70 mV. If pH value is more than 10.30 or less than 4.96, then the zeta potential of particle surface and electrostatic repulsion force decreases due to compression of electrical double layer. Therefore, the suspension exhibits a poorer dispersion.

For Al–Cu alloy powder with the presence of surfactant, the zeta potential is zero at pH 3.80 which is the isoelectric point as shown in Fig. 8. At pH 9.50, the zeta potential is maximum; the electrostatic repulsion force between particles is stronger, and the coagulated particles can redisperse through mechanical force. Therefore the dispersion stability of Al–Cu is best at pH 9.50 corresponding to zeta potential value of −90.60 mV. If pH value is more than 9.50, then the zeta potential of particle surface and electrostatic repulsion force decreases due to compression of electrical double layer. Therefore, the suspension exhibits a poorer dispersion.

3.2.1. Mechanism of dispersion stability

The stability of the ultrafine particles in base fluid during the preparation of suspension is very crucial. Except for the use of ultrasonic equipment, some other techniques such as control of pH or addition of surface active agents are also used to attain stability of the suspension of the nanofluids against sedimentation. These methods change the surface properties of the suspended particles and thus suppress the tendency to form particle clusters. It should be noted that the selection of surfactants should depend mainly on the properties of the solutions and particles.

Oleic acid $CH_3(CH_2)_7CH{=}CH(CH_2)_7COOH$ is a monounsaturated omega-9 fatty acid which is diphilic in nature, i.e. it contains a polar (hydrophilic) and nonpolar (hydrophobic) part. According to dissolving rule (like dissolves like), when oleic acid is added to de-ionized water, the hydrophobic part of oleic acids is attracted to each other and hydrophilic part of oleic acid is concentrated out wards, i.e. hydrophilic part forms polar bond with water molecule. As a result, the oleic acid increases the surface tension of water which prevents the agglomeration of Al–Cu alloy particles when added to de-ionized water. The formation of miscelle of oleic acid in de-ionized water is shown in Fig. 9.

4. Summary and conclusions

The following conclusions can be drawn from the present investigation.

It is possible to prepare ultrafine Al–Cu particles through mechanical alloying process by 50 h of planetary ball milling.

In case of mixture of Al and Cu powder, the alloy formation starts after 10 h of milling. The crystallite size decreases and internal strain increases with milling time up to about 50 h.

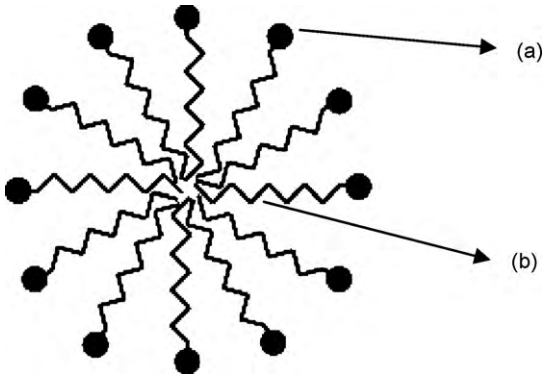

Fig. 9. Schematic diagram represents the formation of miscelle of oleic acid in de-ionized water: hydrophilic (a) and hydrophobic (b) part.

It is found that particle size is around 200–300 nm and crystallite size is around 6 nm and lattice strain is 1.434%.

The dispersion stability of Al–Cu ultrafine particles in base fluid is best at pH value of 4.96, 10.30 corresponding to the zeta potential values of 49.00, −27.7 mV without the presence of surfactant respectively.

In the presence of surfactant, the dispersion stability of Al–Cu ultrafine particles in base fluid is best at pH value of 9.50 corresponding to the zeta potential value of −90.60 mV.

Acknowledgements

The authors would like to thank Prof. S.K. Pratihar and Prof. R. Mazumdar of Ceramic Engineering Department, NIT Rourkela, India for their fruitful discussions in this work.

References

[1] S.U.S. Choi, America Society of Mechanical Engineers (ASME) 66 (1995) 99–105.
[2] H. Masuda, A. Ebata, K. Teramae, K. Hishiunma, Netsu Busei (Japan) 4 (1993) 227–233.
[3] M. Chopkar, S. Kumar, D.R. Bhandari, P.K. Das, I. Manna, Material Science and Engineering B 139 (2007) 141–148.
[4] M. Chopkar, P.K. Das, I. Manna, Scripta Materialia 55 (2006) 549–552.
[5] S. Lee, S.U.S. Choi, S. Li, J.A. Eastman, ASME Journal of Heat Transfer 121 (1999) 280–289.
[6] J.A. Eastman, S.U.S. Choi, S. Li, W. Yu, L.J. Thompson, Applied Physics Letters 78 (2001) 718–720.
[7] S.U.S. Choi, Z.G. Zhang, W. Yu, F.E. Lockwood, E.A. Grulke, Applied Physics Letters 79 (2001) 2252–2254.
[8] S.K. Das, N. Putra, P. Thiesen, W. Roetzel, Journal of Heat Transfer 125 (2003) 567–574.
[9] D.W. Zhou, International Journal of Heat & Mass Transfer 47 (2004) 3109–3117.
[10] T.K. Hong, H.S. Yang, C.J. Choi, Applied Physics Letters 97 (1999) 280.
[11] T.T. Tsung, C.H. Lo, C.S. Jwo, H. Chang, K.C. Wang, International Journal of Advanced Manufacturing Technology 29 (2006) 99–104.
[12] C.H. Lo, T.T. Tsung, L.C. Chen, Journal of Crystal Growth 277 (2005) 636–642.
[13] W. Patungwasa, J.H. Hodak, Materials Chemistry & Physics 108 (2008) 45–54.
[14] W. Zhang, X. Qiao, J. Chen, H. Wang, Journal of Colloid Interface Science 302 (2006) 370–373.
[15] H.E. Patel, S.K. Das, T. Sundararajan, A.S. Nair, B. George, T. Pradeep, Applied Physics Letters 83 (2003) 2931–2933.
[16] G. Gnanaprakash, J. Philip, B. Raj, Materials Letters 61 (2007) 4545–4548.
[17] G. Gnanaprakash, S. Mahadevan, T. Jayakumar, P. Kalyanasundaram, J. Philip, B. Raj, Materials Chemistry and Physics 103 (2007) 168–175.
[18] G. Gnanaprakash, S. Ayyappan, T. Jayakumar, J. Philip, B. Raj, Nanotechnology 17 (2006) 5851–5857.
[19] R.V. Kumar, Y. Diamant, A. Gedanken, Chemistry of Materials 12 (2000) 2301–2305.
[20] V.S. Gurin, A.A. Alexeenko, S.A. Zolotovskaya, K.V. Yumashev, Materials Science Enginering C 26 (2006) 952–955.
[21] S. Li, Z. Hui, J. Yujie, Y. Deren, Nanotechnology 15 (2004) 1428.
[22] B.S. Murty, S. Ranganathan, International Materials Review 43 (1998) 101–141.
[23] T.R. Malow, C.C. Koch, Acta Materialia 46 (1998) 6459–6473.
[24] H. Gleiter, Acta Materials Reviews 48 (2000) 1–29.
[25] C. Suryanarayana, International Materials Review 40 (1995) 41–64.
[26] H. Gleiter, Progress in Material Science 33 (1989) 223–315.
[27] H. Yujin, Jae-K. Lee, J.-K. Lee, Y.M. Jeong, S. Cheong, Y.C. Ahn, S.H. Kim, Powder Technology 186 (2008) 145–153.
[28] H. Chang, Y.C. Chang, Journal of Materials Processing Technology 207 (2008) 193–199.
[29] K. Kwak, C. Kim, Korea-Australia Rheology Journal 17 (2005) 35–40.